DOI 10.1007/s10598-015-9287-9

Computational Mathematics and Modeling, Vol. 26, No. 4, October, 2015

NUMERICAL MODELING OF HEAT AND MOISTURE DIFFUSION IN POROUS MATERIALS

G. P. Vasil'ev,[1] V. A. Lichman,[2] N. V. Peskov,[3] and N. L. Semendyaeva[4] UDC 620.9.697

The article describes a one-dimensional model of heat and moisture transfer in a building wall constructed from several layers of different porous materials. The model consists of a system of diffusion equations for heat, water vapor, and liquid water allowing for condensation of vapor and evaporation of water. An algorithm and a computer program are developed for numerical solution of the model equations by the finite-difference method. Two examples are given calculating the heat and moisture regime of constructions over a 50-year period with allowance for seasonal changes of temperature and air humidity.

Keywords: moisture transfer in a multilayer wall, moisture condensation and evaporation, numerical modeling

1. Introduction

Mass transfer in capillary-porous media over the long term is a topic of both theoretical and experimental research. Classical studies in this field were carried out in the first half of the 20th century [1]. The study of moisture transfer in porous materials is of considerable practical importance as most construction materials have capillary-porous structure. Walls of modern buildings usually consist of several layers of different materials with different physical properties. Under certain conditions, condensation of water vapor may occur near the interface of different materials, leading to formation of liquid moisture (water) in the pore space. The increase in moisture content increases the heat conductivity of the material, thus reducing the thermal resistance of the wall. Moreover, the presence of water in the pore space may destroy the structure of the building material and eventually lead to destruction of the wall.

In Russian building practice, the moisture regime of multilayer walls is commonly calculated using Fokin's phenomenological model [2, 3]. In Fokin's model, the wall interior is divided into two zones, dry and moist; the size of the zones and the boundary between them vary with time. In the dry zone, the moisture is present in the form of adsorbed water firmly bound with the building material and also in the form of water vapor in the pore space. Moisture transfer in the dry zone is possible only through the diffusion of water vapor. The moist zone forms as a result of vapor condensation. In addition to adsorbed water and water vapor, the moist zone also contains liquid water trapped in the pores of the building material. A dynamic equilibrium is assumed to exist in the moist zone between liquid water and water vapor. This implies that the vapor pressure in the moist zone is always equal to the saturated vapor pressure at the given temperature. The moisture concentration in the moist zone changes due to the diffusion of water in the pores, condensation of vapor, and evaporation of water.

Scientific-Research Institute of Moscow Construction, Moscow, Russia; Faculty of Computational Mathematics and Cybernetics, Moscow State University, Moscow, Russia.

[1] E-mail: gpvasiliev@mail.ru.

[2] E-mail: Valitsch@mail.ru.

[3] E-mail: peskov@cs.msu.ru.

[4] E-mail: NatalyS@cs.msu.ru.

Translated from Prikladnaya Matematika i Informatika, No. 47, 2014, pp. 43–59.

Fokin's book [2] gives numerous examples of calculations of the temperature and moisture regime of multilayer walls. The differential equations of the one-dimensional model of heat and moisture diffusion are solved by the method of straight lines on a crude spatial grid using Euler's explicit scheme. Ogniewicz et al. [4] were the first to apply modern computational methods to the problem of simultaneous heat and moisture transfer in a wall built of porous materials. These authors studied the steady-state distribution of heat and moisture in a thermal insulator layer. Their model is essentially similar to Fokin's model. Kohonen [5] was among the first to apply numerical methods to study time-dependent heat and moisture transfer regimes in envelopes of buildings. Kohonen [5] and later studies (see, e.g., [6, 7, 8]) investigated heat and moisture transfer by the finite-difference method, applying more complex models than Fokin's. We should note, however, that model elaboration often involves introduction of new parameters, whose values are unknown, and calculations have to resort to approximate estimates.

Recently, there have been an increasing number of studies modeling the energy balance of a building as a whole with allowance for the effects of both the external and the internal environment. In this case, the model of heat and mass transfer in building envelopes is only a small component of a more general model and therefore should be sufficiently simple and computationally parsimonious [9, 10].

The main objective of the present study is to present a sufficiently accurate and stable numerical algorithm for the solution of Fokin's model on multiprocessor PCs. Our algorithm and computer program can be applied for long-term prediction of the moisture regime with the purpose of optimizing the construction of complex multilayer walls given the climatic conditions in a particular region. Short-term calculations of the moisture regime with allowance for actual climatic data can be applied to interpret the results of thermal testing of buildings, which are usually carried out when construction is completed and some thermophysical characteristics of the walls may substantially deviate from their "equilibrium" values.

The article is organized as follows. Section 2 presents the mathematical formulation of Fokin's model. Section 3 describes the finite-difference scheme and the specific features of the proposed algorithm. In Section 4 we consider two examples computing the moisture regime of a three-layer wall.

2. Model of Moisture Diffusion in the Porous Space

A one-dimensional mathematical model of time-dependent heat and moisture regime of a multilayer building shell has been developed using the Fokin's successive moistening method [2]. The model assumes that inside the wall water can exist in three forms: water vapor, liquid water inside the pore space, and adsorbed water. The adsorbed water is firmly bound with the material particles and is not transported through space. The quantity of adsorbed water per unit volume of the wall material is determined by the relative air humidity inside the pores and is experimentally measurable. Water vapor and liquid water may diffuse through the pore space; the vapor and liquid water flows are assumed proportional to the gradient of vapor pressure and water concentration, respectively. For simplicity, we consider only flows perpendicular to the wall surface.

2.1. Model Parameters. The Ox axis points perpendicularly to the wall surface. The wall of thickness d [m] fills the interval $0 < x < d$ and contains n layers, with d_j the thickness of layer j, $j = 1, 2, \ldots, n$; adjacent layers are made of different materials. The layer boundaries are at the points L_k, $k = 0, 1, \ldots, n$, where $L_0 = 0$, $L_k = \sum_{1 \le j \le k} d_j$, $k > 0$. The material of each wall layer is characterized by the following parameters: ρ [kg/m^3] – density; c [J/(kg·deg)] – specific isobaric heat capacity; λ [W/(m·deg)] – thermal conductivity; μ [g/(hr·m·Pa)] – vapor permeability; β [g/(hr·m·%)] – moisture permeability.

The parameters ρ, c, μ are assumed constant in the relevant range of temperatures and moisture values. The coefficients λ and β in general depend on the temperature T [°C] and the moistness ω [%] of the material (moistness or relative moisture is defined as the ratio of the mass of moisture to the mass of dry material, expressed in percent). In this article we consider only the dependence on moistness, as this parameter varies between wide limits. We thus take $\lambda = \lambda(\omega)$, $\beta = \beta(\omega)$. The specific form of this dependence is determined by polynomial interpolation of experimental data.

The model also uses the experimentally observed dependence of the equilibrium hygroscopic moisture of the material on the relative air humidity and temperature $\omega = o(\varphi, T)$ (for fixed temperature, $\omega = o(\varphi)$ is the sorption isotherm of the material).

2.2. Thermal Conductivity. Heat transfer in each wall layer is described by the heat equation at the corresponding temperature of the material $T(t,x)$ (t is time in hours):

$$c\rho \frac{\partial T(t,x)}{\partial t} = \frac{\partial}{\partial x}\left(\lambda(\omega) \frac{\partial T(t,x)}{\partial x} \right) + Q(T,\omega), \tag{1}$$

where the term Q allows for the latent heat of the vapor–water phase transition (the water–ice phase transition is ignored in the model).

The thermal conductivity $\lambda(\omega(x))$ is a continuous function inside each wall layer with discontinuities at the layer boundaries. Equation (1) is accordingly defined inside the layers, with continuity conditions on temperature and heat flux at the layer boundaries:

$$T(t,x))\big|_{x=L_j-0} = T(t,x))\big|_{x=L_j+0},$$

$$\lambda(\omega) \frac{\partial T(t,x)}{\partial x}\bigg|_{x=L_j-0} = \lambda(\omega) \frac{\partial T(t,x)}{\partial x}\bigg|_{x=L_j+0}, \quad j = 1,2,\ldots,n-1. \tag{2}$$

On the outer surface of the wall, we specify convective heat exchange with the ambient air, whose temperature $T_{\text{ex}}(t)$ is a given function of time:

$$-\lambda(\omega) \frac{\partial T(t,x)}{\partial x}\bigg|_{x=L_0} = \alpha_{\text{ex}} \left(T_{\text{ex}}(t) - T(t,x) \right)\big|_{x=L_0}, \tag{3}$$

where α_{ex} [$\text{W}/(\text{m}^2 \cdot \text{K})$] is the heat exchange coefficient. Similarly, on the inner wall surface we specify convective heat exchange with the inside air:

$$-\lambda(\omega) \frac{\partial T(t,x)}{\partial x}\bigg|_{x=L_n} = \alpha_{\text{in}} \left(T(t,x) - T_{\text{in}}(t) \right)\big|_{x=L_n}. \tag{4}$$

2.3. Vapor Permeability. If the relative air humidity φ in the pores is less than 1, then the material contains only absorbed moisture and water vapor. With relative air humidity $\varphi < 1$ the mass of adsorbed moisture

per unit volume ($1\ m^3$) of the material equals $0.01\omega\rho$, where ρ is the density of the material and ω is the relative moisture in percent; $\omega = o(\varphi)$ is determined from the sorption isotherm for the specific material. In this case, moisture is transported only as water vapor, and its transport is described by the diffusion equation for water vapor at partial pressure $e(t,x)$ [Pa]:

$$\xi(\omega)\rho\frac{\partial e(t,x)}{\partial t} = \mu\frac{\partial^2 e(t,x)}{\partial x^2}. \tag{5}$$

(Thermal diffusion of vapor, i.e., diffusion driven by the temperature gradient, is ignored in the model.) The parameter ξ [g/(kg·Pa)] is the "vapor capacity" of the material; its numerical value can be estimated by the formula [2]

$$\xi(\omega(\varphi)) = \frac{do(\varphi)}{d\varphi}.$$

As noted previously, Eq. (5) is defined on the part of the interval $(0,d)$ where $\varphi < 1$, or $e < E$ (because $\varphi = e(t,x)/E(T)$), where $E = E(T)$ is the saturated water vapor pressure at temperature T. The size and the location of this region vary with time, and we accordingly denote it by $V_t \subset (0,d)$ (the "dry" zone).

If the point L_j, $0 < j < n$, is in V_t, then a pressure and vapor flux continuity condition similar to condition (2) is specified at this point. If the points L_0 and/or L_n are boundary points of the region V_t, then conditions of convective vapor exchange with outside and/or inside air similar to (3), (4) are specified at these points.

2.4. Moisture Permeability. The part of the interval $(0,d)$ not included in V_t is denoted W_t (the "moist" zone), $V_t \bigcup W_t = (0,d)$. In the region W_t the pore space contains both water vapor and liquid water. We assume that water and vapor are in an equilibrium, i.e., the vapor pressure is equal to the saturated vapor pressure at the given temperature, $e(t,x) = E(T(t,x))$. The quantity of liquid moisture w, expressed in percent of the material mass, can be estimated from the equality

$$w(t,x) = \omega(t,x) - o(1), \tag{6}$$

where $o(1)$ is the maximum hygroscopic moisture of the material corresponding to relative air humidity $\varphi = 1$.

Diffusion of liquid moisture in the wet region W_t is described by the equation

$$10\rho\frac{\partial w(t,x)}{\partial t} = \frac{\partial}{\partial x}\left(\beta(\omega)\frac{\partial w(t,x)}{\partial x}\right) + \mu\frac{\partial^2 E(T)}{\partial x^2}. \tag{7}$$

The factor 10 in (7) is associated with the units of measurement of the coefficients β and μ, where mass is in grams, and with the fact that the relative moisture ω is in percent.

As noted previously, we assume dynamic equilibrium of the two phases of water in W_t. Thus, to keep the model simple, we impose impermeability condition (8) on water at the boundary of the regions W_t and V_t,

and also at the points L_0 and/or L_n, if these are boundary points of W_t:

$$\left.\frac{\partial w(t,x)}{\partial x}\right|_{x\in\partial W_t} = 0\,. \tag{8}$$

If any of the points L_j, $0 < j < n$, is in W_t, then at this point we specify continuity of water concentration and water flux similar to conditions (2). Assume that $\overline{x}$ is a boundary point separating the regions V_t and W_t, and for definiteness let the region V_t be to the left of $\overline{x}$. Then at the point $\overline{x}$ we specify the vapor pressure continuity condition

$$e(t,x)\big|_{x=\overline{x}-0} = E(t,x)\big|_{x=\overline{x}+0}\,. \tag{9}$$

2.5. Allowing for Latent Heat of Vapor–Water Phase Transition. In Eq. (7), the term $v = \mu\,\partial^2 E/\partial x^2$ $[\,\mathrm{g/(hr\cdot m^3)}\,]$ is the rate of change of the liquid concentration due to condensation of the vapor or evaporation of the water, i.e., as a result of a phase transition. This change is accompanied by release or absorption (depending on the sign of v) of phase transition heat. This latent heat is allowed for in Eq. (1) by the term Q, whose values are given by the formula

$$Q = \begin{cases} q_L v, & x \in W_t, \\ 0, & x \in V_t, \end{cases}$$

where q_L is the specific heat of phase transition.

3. Numerical Solution

The system of differential equations for the temperature $T(t,x)$ (1), partial water vapor pressure $e(t,x)$ (5), and percent concentration of liquid moisture $w(t,x)$ (7) is numerically solved by the finite-difference method.

The space derivatives are approximated on the interval $(0,d)$ by defining a uniform space grid $x_k = (k-0.5)h$, $k = 1,2,\ldots,N$, $h = d/N$. For simplicity we assume that the layer boundaries (the points L_j, $0 < j < n$) fall precisely in the middle between neighboring grid points. With a sufficiently large N, this assumption clearly does not affect the result.

The time derivatives are approximated on the time grid $t_0(=0)$, $t_1,\ldots,t_m,\ldots$ with a variable increment $\tau_m = t_{m+1} - t_m$, $m \ge 0$. The coefficients of the equations and the unknown functions are approximated by grid functions using the formula $f_k^m = f(t_m, x_k)$. In what follows, for conciseness, we drop the superscript of the grid functions, denoting them as f_k on the current time layer $t = t_m$ and $\hat{f}_k$ (under the hat sign ^) on the next time layer $t = t_{m+1}$.

3.1. Finite-Difference Equations. The system of finite-difference equations of our model is derived from the differential equations by the balance method. Using an implicit scheme to approximate the time derivatives, we obtain a system of difference equations in the form

$$hc_k\rho_k\frac{\hat{T}_k - T_k}{\tau} = \hat{\Lambda}_k^-\left(\hat{T}_{k-1} - \hat{T}_k\right) - \hat{\Lambda}_k^+\left(\hat{T}_k - \hat{T}_{k+1}\right) + \hat{Q}_k, \quad k = 1,2,\ldots,N, \tag{10}$$

$$h\xi_k\rho_k\frac{\hat{e}_k - e_k}{\tau} = \hat{\mathrm{M}}_k^-\left(\hat{e}_{k-1} - \hat{e}_k\right) - \hat{\mathrm{M}}_k^+\left(\hat{e}_k - \hat{e}_{k+1}\right), \quad x_k \in V_t, \tag{11}$$

$$10h\rho_k\frac{\hat{w}_k - w_k}{\tau} = \hat{\mathrm{B}}_k^-\left(\hat{w}_{k-1} - \hat{w}_k\right) - \hat{\mathrm{B}}_k^+\left(\hat{w}_k - \hat{w}_{k+1}\right) + \hat{v}_k, \quad x_k \in W_t. \tag{12}$$

The coefficients Λ are calculated from

$$\Lambda_1^- = \frac{2\alpha_{ex}\lambda_1}{\alpha_{ex}h + 2\lambda_1}, \quad \Lambda_k^- = \frac{2\lambda_{k-1}\lambda_k}{h\left(\lambda_{k-1} + \lambda_k\right)}, \quad k = 2,\ldots,N,$$

$$\Lambda_k^+ = \frac{2\lambda_k\lambda_{k+1}}{h\left(\lambda_k + \lambda_{k+1}\right)}, \quad k = 1,\ldots,N-1, \quad \Lambda_N^+ = \frac{2\lambda_N\alpha_{in}}{2\lambda_N + \alpha_{in}h}.$$

The formulas for the coefficients M and B have the same form with an obvious change of variables. We should note that the coefficients B are calculated only in the region W_t, and we always have $\mathrm{B}_1^- = 0$ and $\mathrm{B}_N^+ = 0$.

$$v_k = \mathrm{M}_k^-\left(E_{k-1} - E_k\right) - \mathrm{M}_k^+\left(E_k - E_{k+1}\right),$$

where $E_j = E(T_j)$ if $x_j \in W_t$; and $E_j = e_j$ if $x_j \in V_t$, $j = k-1, k, k+1$.

Setting $T_0 = T_{\mathrm{ex}}(t_m)$, $T_{N+1} = T_{\mathrm{in}}(t_m)$, and $e_0 = e_{\mathrm{ex}}(t_m)$, $e_{N+1} = e_{\mathrm{in}}(t_m)$, we obtain a closed system of 2N nonlinear algebraic equations (10)–(12) in $2N$ unknowns.

3.2. Solution by Iteration. System (10)–(12) can be solved by iteration. Assume that the solution T, e, w at time t_m is known (for t_0 use the initial condition). Use the solution T, e, w to evaluate the coefficients Λ, M, B. Substituting these coefficients in system (10)–(12), we obtain a system of linear equations in $\hat{T}$, $\hat{e}$, $\hat{w}$. The solution of the linear system $T^{(1)}$, $e^{(1)}$, $w^{(1)}$ constitutes the first approximation to the solution $\hat{T}$, $\hat{e}$, $\hat{w}$.

In the second iteration, apply the first approximation to evaluate the coefficients. The solution of the linear system obtained in this way constitutes the second approximation $T^{(2)}$, $e^{(2)}$, $w^{(2)}$ to the solution of the original system. Continuing the iterations, we obtain a sequence of approximations $\left\{T^{(i)}, e^{(i)}, w^{(i)}\right\}$ to the solution $\hat{T}$, $\hat{e}$, $\hat{w}$. The iterations stop when the Euclidean norms of the difference between two successive approximations $\left\|T^{(i)} - T^{(i-1)}\right\|$, $\left\|e^{(i)} - e^{(i-1)}\right\|$, and $\left\|w^{(i)} - w^{(i-1)}\right\|$ become sufficiently small.

If the convergence condition is not satisfied after a given maximum number of iterations, the current iteration is stopped and the time step is judged as failed. In this case, the time increment τ is reduced and a new iteration loop starts. If the convergence condition is satisfied in fewer than the maximum number of iterations,

the iterations are stopped and the time step is judged successful (see Sec. 3.4). The current time is incremented by τ.

The linear equation systems for temperature (10) and moisture (11), (12) are independent in each iteration, and they can be solved in parallel on different processors in multiprocessor PCs.

3.3. Redetermination of the "Wet" Zone. Note that all the iterations in one time step are executed with fixed regions V_t and W_t. The "wet" (and thus also the "dry") zone are redetermined after each successful time step.

Initially at time $t_0 = 0$, the "wet" region W_0 includes all points where the relative moisture is not less than the maximum hygroscopic moisture.

After each successful time step m, W_m is augmented with the points $x_k \in V_m$ where the vapor pressure has become not less than the saturated vapor pressure ($e_k \geq E(T_k)$). Water concentration at the point x_k is taken equal to $w_k = \tilde{o}(\varphi)$, where $\tilde{o}$ is the extrapolation of the sorption isotherm o to values $\varphi > 1$. The water vapor pressure at the point x_k is taken equal to the saturated water vapor pressure at the temperature T_k, $e_k = E(T_k)$.

The points $x_k \in W_m$ where water concentration drops below zero ($w_k < 0$) are excluded from W_m and included in V_m. The relative moisture at the point x_k is set equal to $\omega_k = o(1) - w_k$, and the water vapor pressure is determined by solving the equation $o(\varphi) = \omega_k$.

New zones V_{m+1} and W_{m+1} are thus formed. No restrictions are imposed on the shape and size of the "wet" zone: both the "wet" and the "dry" zone may contain intervals and/or isolated points.

3.4. Choice of Time Increment. The heat and moisture transfer model described above is intended for modeling the heat and moisture regime of a wall over a long time, usually several years. During this period, "wet" zones in the wall may appear and disappear several times. A "wet" zone usually forms during the cold time of the year and disappears (dries) during the warm season. In periods without qualitative changes in the moisture regime (summer, winter), the integration increment τ may be relatively large. Conversely, in seasons when a "wet" zone appears and disappears (autumn, spring), the increment τ should be relatively small to ensure stability of the difference scheme. Efficient functioning of the algorithm therefore requires varying the increment in accordance with the properties of the solution.

In the computer program, the increment τ is varied by a simple procedure, which is both important and effective. Initially, τ is taken sufficiently small compared with the given maximum increment $\tau_{\max}$. For instance, we may take $\tau = 0.001\tau_{\max}$. A time step with a given τ is judged "successful" if

(a) the number of iterations to satisfy the convergence condition does not exceed the maximum number of iterations and

(b) the relative changes in the solution norm in one step do not exceed a given (sufficiently small) value. More precisely, the following inequalities are required to hold:

$$\left\|\hat{T} - T\right\| < \varepsilon_1^T \|T\| + \varepsilon_2^T, \quad \|\hat{e} - e\| < \varepsilon_1^e \|e\| + \varepsilon_2^e, \quad \|\hat{w} - w\| < \varepsilon_1^w \|w\| + \varepsilon_2^w.$$

If the step "fails", τ is reduced by a given proportion and a new attempt is made with the new τ. This process continues until the step become "successful", or until τ become smaller than the given minimum val-

ue $\tau_{\min}$. In the latter case, the program halts. The increment is increased if the current value does not exceed $\tau_{\max}$ and the number of successive successful steps is greater than a given value.

4. Computation Examples

In this section we present two examples that compute the moisture regime of a three-layer wall consisting of two materials: concrete (strength) and mineral wool (thermal insulation). The three layers are arranged in the following order inside the wall: concrete–mineral wool–concrete. The wall thickness is $d = 0.4$ m. We consider two alternative wall constructions. Case A: $d_1 = 0.1$ m, $d_2 = 0.1$ m, $d_3 = 0.2$ m; case B: $d_1 = 0.2$ m, $d_2 = 0.1$ m, $d_3 = 0.1$ m. In construction A, the insulation is closer to the outside surface of the wall; in construction B, conversely, it is closer to the inside surface of the wall.

4.1. Characteristics of Wall Materials. In our calculations we used typical parameter values that could be found in standard construction handbooks (Table 1). In particular, we used the data from [2, 3]. The values of some parameters in the reference literature are traditionally given in technical units. These parameters have been converted to SI units.

Table 1. Parameter Values

	Concrete (on crushed brick)	Mineral wool
ρ, kg/m^3	2400	150
c, kJ/(kg·deg)	0.84	0.84
μ, g/(hr·m·Pa)	$3.0 \cdot 10^{-5}$	$3.1 \cdot 10^{-4}$
λ_0, W/(m·deg)	1.51	0.038
k_λ, W/(m·deg·%)	0.1164	0.0017
β_0, g/(m·hr·%)	0.01	$2.65 \cdot 10^{-6}$
k_β, g/(m·hr·%·%)	0.018	$8.18 \cdot 10^{-6}$

We assume that the thermal conductivity λ and moisture permeability β are linear functions of the relative moisture of the material: $\lambda = \lambda_0 + k_\lambda \omega$, $\beta = \beta_0 + k_\beta w$. (In calculations, we measure power in units of kJ/hr, 1 W = 1 J/sec = 3.6 kJ/hr)

In Fig. 1, the markers plot the handbook data from [3] and the curves are polynomial interpolation of the data. The sorption isotherm for concrete is given by the polynomial

$$o_c(\varphi) = 0.65\varphi^2 + 0.70\varphi + 0.04 .$$

The maximum hygroscopic moisture of concrete is $o_c(1) = 1.39$ %.

For mineral wool,

$$o_w(\varphi) = 6.643\varphi^4 - 8.990\varphi^3 + 3.755\varphi^2 + 0.007\varphi + 0.013 .$$

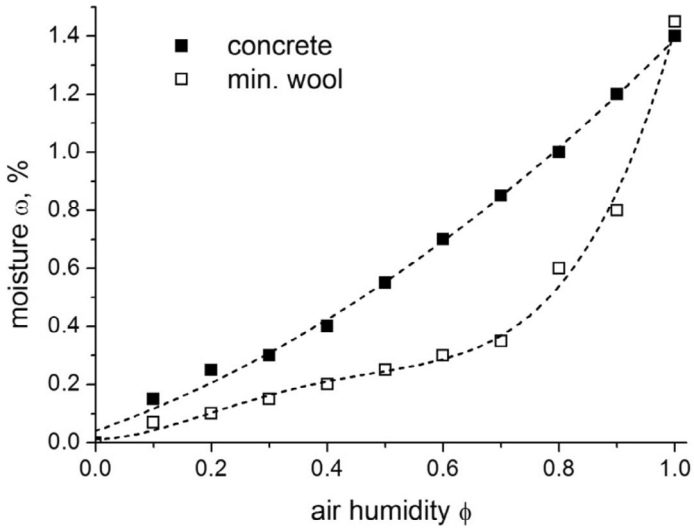

Fig. 1. Sorption isotherm $o(\varphi)$ of concrete and mineral wool.

The maximum hygroscopic moisture of mineral wool is $o_w(1) = 1.43\,\%$.

Convective heat exchange between the wall and ambient air (3), (4) is determined by the heat transfer coefficients on the outer wall surface $\alpha_{ex} = 23$ kcal/($m^2 \cdot$ deg) and on the inner wall surface $\alpha_{in} = 7.3$ kcal/($m^2 \cdot$ deg) (1 kcal = 4.1868 kJ). The resistance to moisture transfer on the outer and the inner wall surface is set equal to 0.1 and 0.2 (mm Hg·hr· m^2)/g, respectively [2] (1 mm Hg = 133.322 Pa).

4.2. Climatic Data. Seasonal variations of temperature and air humidity are modeled using monthly average values of these parameters as observed in the Moscow region. Daily average values of T_{ex} and φ_{ex} were determined by Fourier interpolation of the monthly data.

Table 2. Monthly Average Temperature and Relative Air Humidity

	Jan	Feb	Mar	Apr	May	Jun	Jul	Aug	Sep	Oct	Nov	Dec
T_{ex}, °C	–9.4	–8.5	–3.6	4.9	12.9	17.0	19.3	17.4	11.7	5.0	–1.6	–6.9
φ_{ex}	0.84	0.81	0.78	0.65	0.58	0.59	0.63	0.68	0.73	0.78	0.82	0.85

The temperature and the relative air humidity in the internal space were assumed constant: T_{in} = 20°C, φ_{in} = 0.55.

4.3. Initial Conditions. Mid-July is the initial time in our calculations. At this time, the external air temperature is $T_{ex}(t_0) = 19.3°\,\mathrm{C}$ and the internal air temperature is $T_{in}(t_0) = 20°\,\mathrm{C}$. Initially, the wall temperature is assumed constant over the entire thickness, equal to $T(t_0, x) = \left(T_{ex}(t_0) + T_{in}\right)/2$.

The initial moisture of both concrete and mineral wool is assumed 1% by weight, which is less than the maximum hygroscopic moisture of these materials. Thus, initially there is no liquid water in the wall (i.e., no

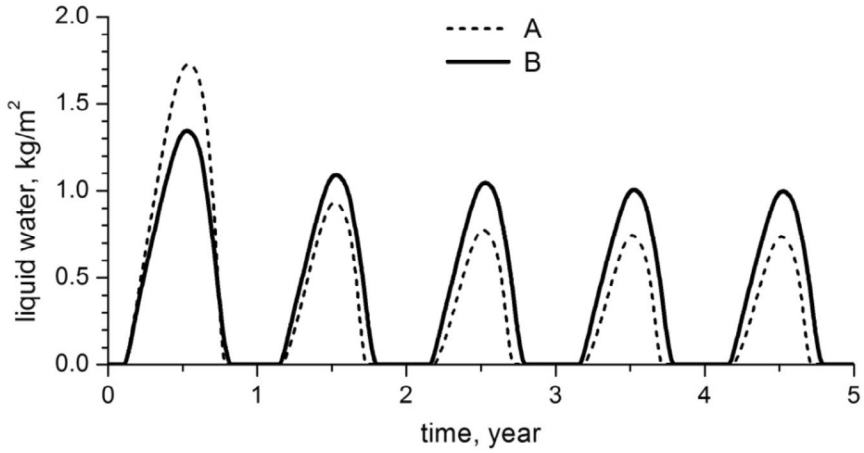

Fig. 2. Liquid water mass per $1\,\mathrm{m}^2$ of wall surface in cases A and B

"wet" zone, $W_0 = \varnothing$). Given the initial moisture, we use the sorption isotherm of the corresponding material to find the initial relative air humidity in the pore space and then compute the initial partial pressure of water vapor.

The relative air humidity φ and the partial water vapor pressure e at temperature T are related by the equality $\varphi = e/E(T)$, where $E(T)$ is the saturated water vapor pressure. We evaluate $E(T)$ from the approximate formula

$$E(T) = \begin{cases} 4.688\,(1.486 + T/100)^{12.3}, & T < 0, \\ 288.58\,(1.098 + T/100)^{8.02}, & T \geq 0. \end{cases}$$

4.4. Computation Results. The heat and moisture regime of the wall in cases A and B has been calculated for a period of 5 years.

Figure 2 plots the mass of liquid water per $1\,\mathrm{m}^2$ of wall surface during five years (each year starts in mid-July). We conclude from the graphs that moisture condensation occurs in the wall each year from October to April. In steady state, the liquid water mass in wall A is approximately 20% less than in wall B, but in both cases the liquid water mass per $1\,\mathrm{m}^2$ of wall surface does not exceed 1 kg. In these constructions, the mass of 1 m^2 of dry wall is 735 kg.

Figure 2 shows that the first two years are characterized by a transient process in the wall, with initial moisture deviating from the "equilibrium" state. With initial moisture of 1%, the wall material is "overmoist", and the wall gradually dries during the first two years – the excess moisture is removed. Figure 3 shows the vapor flux through the external wall surface. Negative values correspond to vapor flux from the wall to the outside air; positive values correspond to flux from outside air into the wall. Phase transitions in pore moisture, vapor condensation and water evaporation, are accompanied by release and absorption of heat. Figure 4 plots the phase transition heat during one day per $1\,\mathrm{m}^2$ of wall surface. Positive values correspond to heat release (during condensation); negative values correspond to heat absorption (during evaporation).

The next three figures show the space-time diagrams of wall temperature, relative air humidity in the pores, and liquid water mass in the pores. The diagrams illustrate the evolution of the corresponding variables during year 5, when the annual wall temperature and wall moisture values have stabilized.

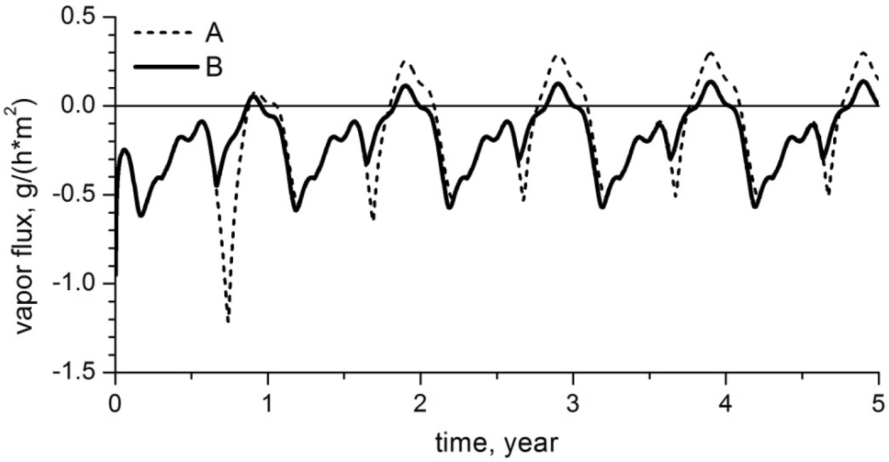

Fig. 3. Water vapor flux through the external wall surface.

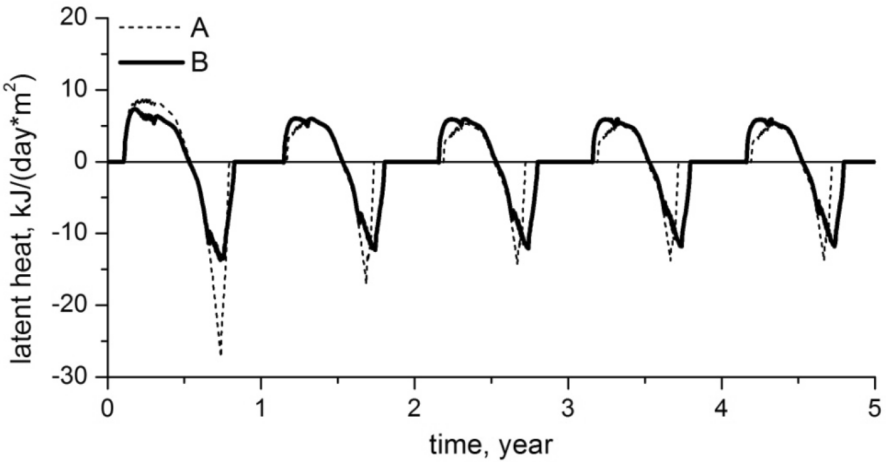

Fig. 4. Latent heat of pore moisture per 1 m^2 of wall surface during one day

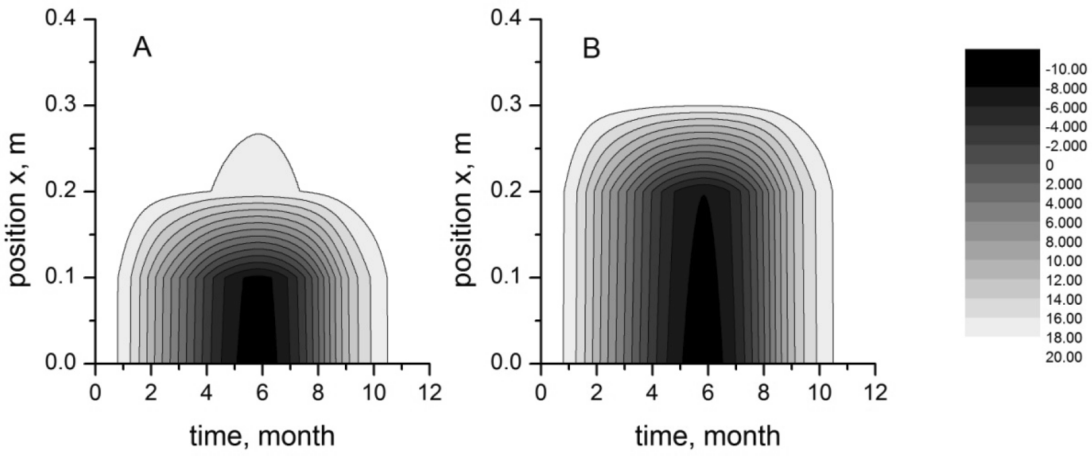

Fig. 5. Space-time diagram of temperature (centigrade).

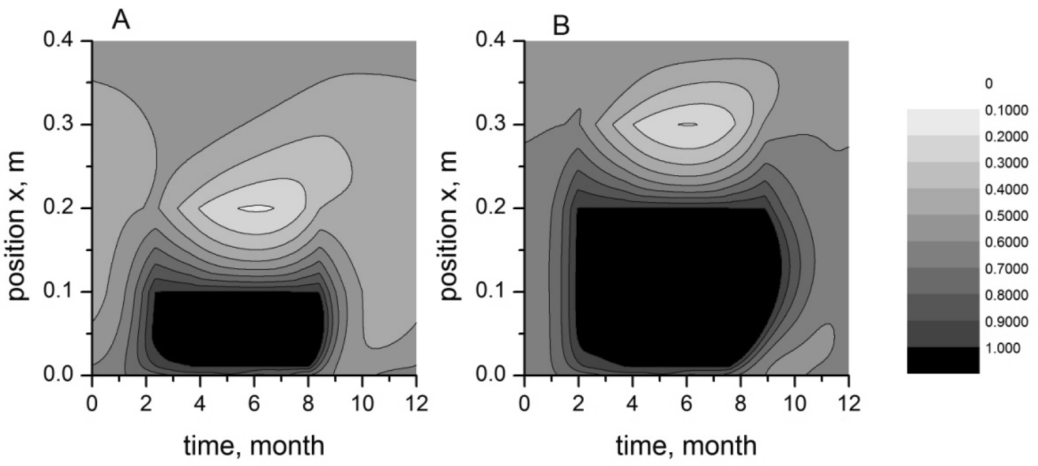

Fig. 6. Space-time diagram of relative air humidity in the pores.

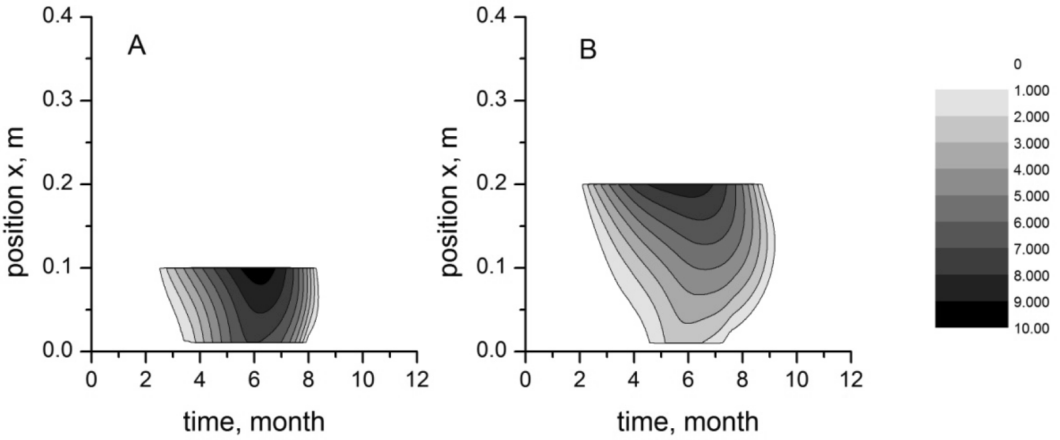

Fig. 7. Space-time diagram of liquid water concentration [kg/m^3].

The temperature space-time diagram in Fig. 5 shows that the main temperature changes in the wall occur in the thermal insulation layer, while the temperature in the concrete layers does not change much.

Vapor condensation is observed in the outer concrete layer and in the adjoining insulation layer, where the temperature repeats the annual variation of external air temperature. During the cold season, the water vapor pressure in the pores exceeds the saturated vapor pressure and condensation of vapor begins. In wall B, the condensation region is twice as wide as in wall A, so that more water is formed in wall B (Fig. 2).

The diagram of relative air humidity in the pores of the wall material (Fig. 6) shows the "wet" zone (colored black), where the relative air humidity equals 1.

From the diagram of liquid water concentration in Fig. 7 we see that the maximum concentration of moisture in the external concrete layer is observed near the contact surface with the thermal insulation layer.

Thus, the closer the insulation layer to the outer wall surface, the narrower is the water vapor condensation zone and the smaller is the liquid water mass forming inside the wall during the cold time of the year. This is a well-known fact in construction practice. Our examples demonstrate the computational potential of Fokin's model and our numerical program.

5. Conclusion

The article presents a finite-difference scheme and a numerical algorithm for Fokin's model of time-dependent heat and moisture transfer in a multilayer wall built of different porous materials. Parallel solution of the heat and moisture transfer equations and the use of a variable time increment essentially reduce processor time. The proposed computer program can be used in applied engineering calculations for long-term prediction of the moisture regime in multilayer walls with allowance for climatic conditions. The examples presented in the article demonstrate the computational capabilities of the program.

Research supported by the Russian Ministry of Education and Science (grant RFMEFI57614X0034).

REFERENCES

1. A. V. Lykov, *Transfer Phenomena in Capillary-Porous Bodies* [in Russian], Gostekhteoretizdat, Moscow (1954).
2. K. F. Fokin, *Thermal Engineering of Building Walls* [in Russian], Stroiizdat, Moscow (1973).
3. *Handbook for Calculation of the Moisture Regime of Building Walls* [in Russian], Stroiizdat, Moscow (1984).
4. Y. Ogniewicz and C. I. Tien, "Analysis of condensation in porous insulation," *Int. J. Heat Mass Transfer,* **24**, 421–429 (1981).
5. R. Kohonen, "Transient analysis of the thermal and moisture physical behaviours of building constructions," *Building and Environment,* **19**, 1–11 (1984).
6. H. M. Kiinzel and K. Kiessl, "Calculation of heat and moisture transfer in exposed building components," *Int. J. Heat Mass Transfer,* **40**, 159–617 (1997).
7. P. Haupl, J. Grunewald, H. Fechner, and H. Stopp, "Coupled heat air and moisture transfer in building structures," *lnt. J. Heat Mass Transfer,* **40**, 1633–1642 (1997).
8. N. Mendes, F. C. Winkelmann, R. Lamberts, and P. C. Philippi, "Moisture effects on conduction loads," *Energy and Buildings,* **35**, 631–644 (2003).
9. X. Fanga, A. K. Athienitis, and P. P. Fazio, "Methodologies for shortening test period of coupled heat-moisture transfer in building envelopes," *Applied Thermal Engineering,* **29**, 787–792 (2009).
10. M. Steeman, A. Janssens, H. J. Steeman, M. Van Belleghem, and M. De Paepe, "On coupling 1D non-isothermal heat and mass transfer in porous materials with a multizone building energy simulation model," *Building and Environment,* **45**, 865–877 (2010).